The extended disordered sequences in ribosome-associated germline-specific NAC proteins are their feature compared to the ubiquitously expressed paralog

Galina L. Kogan
NRC “Kurchatov Institute” - Institute of Molecular Genetics
Elena A. Mikhaleva
NRC “Kurchatov Institute” - Institute of Molecular Genetics
Oxana M. Olenkina
NRC “Kurchatov Institute” - Institute of Molecular Genetics
Sergei S. Ryazansky
NRC “Kurchatov Institute” - Institute of Molecular Genetics
Oxana V. Galzitskaya
Institute of Theoretical and Experimental Biophysics
Yuri A. Abramov
NRC “Kurchatov Institute” - Institute of Molecular Genetics
Toomas A. Leinsoo
NRC “Kurchatov Institute” - Institute of Molecular Genetics
Natalia V. Akulenko
NRC “Kurchatov Institute” - Institute of Molecular Genetics
Sergei A. Lavrov
NRC “Kurchatov Institute” - Institute of Molecular Genetics
Vladimir A. Gvozdev (gvozdev@img.ras.ru)
NRC “Kurchatov Institute” - Institute of Molecular Genetics

Article

Keywords:

Posted Date: March 14th, 2022

DOI: https://doi.org/10.21203/rs.3.rs-1430778/v1

Abstract

The nascent polypeptide-associated complex (NAC) consisting of α- and β-subunits is an essential conserved ribosome-associated protein in eukaryotes. NAC is considered as a ubiquitously expressed co-translational regulator of nascent protein folding and sorting providing homeostasis of cellular proteins. Here we discovered the germline-specific NACαβ paralogs (gNACs), whose β-subunits, non-distinguishable by ordinary immunodetection, being encoded by five highly homologous gene copies while α-subunit is encoded by the single *αNAC* gene. Immunostaining detects the gNAC expression in the primordial embryonic and adult gonads. The germline specific α and β subunits differ from the ubiquitously expressed paralogs by the acquisition of extended intrinsically disordered regions (IDRs) at the N- and C-ends of coding regions, respectively, which were predicted to be phosphorylated. The presence of distinct phosphorylated isoforms of gNAC-β subunits is confirmed by comparison of their profiles by 2D-isoeletrophocusing resolution before and after phosphatase treatment of testis ribosomes. We propose IDR-dependent molecular crowding and specific coordination of the NAC and other proteostasis regulatory factors in the ribosomes of germinal cells. A possibility of the functional crosstalk's between the germinal and ubiquitous α- and β- subunits is revealed by assessing their depletion effects on the fly viability and gonad development.

Summary

The ubiquitously expressed nascent polypeptide-associated complex (NAC) consisting of α- and β-subunit is a ribosome associated protein involved in proteostasis. The evolutionary conserved germinal cell-specific paralogs of NAC carrying extended disordered regions and being prone to phosphorylations are detected in *Drosophila melanogaster*

Introduction

The evolutionary conservative NAC (nascent polypeptide associated complex consisting of α and β subunits) interacts with translating ribosomes and functions as a ubiquitous ATP-independent chaperone in eukaryotes [1,2]. It is suggested that the majority of the translating ribosomes are associated with NAC [3,4]. NAC is involved in co-translational protein folding [5] and delivery of mitochondrial precursor proteins [6]. Recently, new mechanistic insights were achieved in the studies of NAC-β subunit function by the demonstration that N-terminal of NAC-β subunit is able to be inserted deeply into the ribosomal tunnel, close to polypeptide transferase center, to sense nascent polypeptide [7]. The sensing NAC-β ability is coupled with its flexibility and conformational switches that either activate or prevent its alternative associations with the translocon complex of the endoplasmic reticulum (ER) or signal recognizing particle (SRP). These conformational changes of flexible NAC structure are suggested to regulate correct protein sorting for membrane components or secretion. NAC modulates protein transmission to ER lumen or cytosol, ensuring a specific co-translational protein biogenesis pathway [1–3,8].

Here we have focused on the specific paralogs of NAC-β and NAC-α proteins expressed in the germ cells in *D. melanogaster*. Earlier, for the first time to our knowledge, we have discovered the expression of tissue specific NAC subunit in eukaryotes, detecting testis-specific amplified βNAC paralogs designated as the βNACtes genes (see FlyBase.org data and [9]). The amplified βNACtes genes were found in the genomes of sister species, *D. melanogaster* and *D. simulans*, but not in closely related *D. yakuba*, [9]. The generation of rat anti-NACtes Abs allowed us to reveal exclusively germinal, mostly spermatocyte expression of the βNACtes genes [10]. Here we further extended these studies by detecting the germinal NAC-α subunit as a product of the unique gene *CG4415* in the *D. melanogaster* genome thus proving the existence of the germline specific heterodimeric NAC-αβ, gNACs. We also showed that both germinal α- and β-subunits differ from ubiquitously expressed paralogs by the acquirement of extensive intrinsically disordered regions (IDRs), primarily at the N- and C-ends, respectively. The IDRs are known to be important chaperone functional regions [11,12] and their significant length increase in gNAC may indicate a complex role for IDRs in the detection of conformational switches of clients in germ cells. Albeit functions of gNAC are still mysterious, it is believed that acquired extended IDRs are generally prone to extensive post-translational modifications (PTMs) [13] as well as to the implementation of protein-protein interactions [14]. The germinal βNAC subunit was shown to be accumulated in ribosomes [10]. The 2D-electrophoresis with isoelectric focusing of testis ribosomal extract followed by specific immunostaining revealed a set of resolved spots of gNAC-β isoforms. The phosphatase treatment diminished the negative charges of these isoforms, indicating the presence of predicted gNAC-β phosphorylation.

Results

Detection of the germ cell-specific α- and β-paralogs forming the heterodimeric germinal NAC

Earlier, we have annotated five paralogs of ubiquitously expressed β-subunit of NAC (*bic*) gene [9] represented by two pairs of adjacent genes at the 12E8-9 region of the X-chromosome of *D. melanogaster* (Flybase.org and [15,16]) and a single gene outside in 12E2 [15,17]. The gene *CG4415* (located at the tip of 2L chromosome, 21E3) encodes α-NAC domain and was shown to be expressed in the embryonic gonads (BDGP *in situ* homepage data, https://insitu.fruitfly.org). Moreover, a network analysis of protein-protein interactions using the String database (v. 10.5) [18] indicated the putative physical interaction of NAC-βtes4 with *CG4415* gene product (NAC-α subunit). To directly demonstrate the heterodimerization of the putative germinal α-NAC and β-NACtes subunits, we performed co-transfection of S2 somatic *D. melanogaster* cells lacking the expression of germinal β-subunit with two plasmids encoding Flag-tagged gNAC-β (NAC-βtes4) and HA-tagged gNAC-α subunits. The complete colocalization of FLAG-gNAC-β and HA-gNAC-α indicates the formation of germinal gNACαβ-heterodimer (Fig. 1a). The putative heterodimer was immunoprecipitated using anti-FLAG or anti-HA Abs and subsequent WB-analysis confirmed the interaction of FLAG-gNAC-β and HA-gNAC-α subunits (Fig. 1b). Taking into account the detection of the *CG4415* gene transcripts in the embryonic primordial gonads by *in situ* hybridization (Fig. 1c, from BDGP

in situ homepage), we also confirmed the presence of βNACtes protein in the germline tissues of embryos by immunostaining with βNACtes Abs (Fig. 1d-i). The similar distribution of both gNAC-α mRNA and βNACtes subunits in the primordial embryonic gonad (Fig. 1c, d) allows us to use further the gNAC designation for heterodimeric germline-specific NAC proteins, containing a single definite germinal NAC-β subunit, earlier termed as βNACtes [10] and the newly detected here gNAC-α subunit. The clusters of embryonic germinal cells migrating to attach to primordial somatic gonadal cells were detected using immunostaining for the germinal VASA marker and the gNAC-β (Fig. 1, e-g). In accordance with our earlier observations [10], we've found the strong gNAC-β expression in testis spermatocytes, but not in somatic testis accessory glands (Fig. 1,h, arrow) as well as gNAC-β accumulation at the late stage of oogenesis in the germ plasm at the posterior pole of the mature egg (Fig. 1,i) [19,20].

The germinal α- and β-subunits are enriched with IDRs

The study of the conformation of the ubiquitously expressed NAC from *Caenorhabditis elegans* revealed its flexibility ensuring its ability to bind various protein substrates, irrespective of whether they are folded or intrinsically disordered [21]. The discovery of the germline paralogs of both NAC subunits prompts us to compare the predicted conformational flexibility of their sequences with ubiquitous paralogs by assessing the IDRs outside the folded NAC domains known to handle αβ dimerization. The profiles of the disordered regions were obtained using the IsUnstruct program [22,23] (Fig. 2). The both ubiquitous and germinal α-subunits contain the NAC-domain and the ubiquitin-activated domain (UBA), which was recently shown as the SRP interactor, stabilizing the co-binding of SRP and NAC on the signal-sequence displaying ribosomes [8]. The germinal α-subunit has an approximately three-fold increase in IDR length at the N-terminus in comparison with the ubiquitous paralog. The ubiquitous β-subunits carry a conserved positively charged motif at the N-end of the ribosome associated region [1] and the NAC dimerizing domain, while germinal paralog preserving this charged motif has a more than twofold increase in IDR length at the C-terminus. Thus, a significant difference in amino acid sequence patterns between the germinal and ubiquitous subunits lies in the extensions of germinal-specific IDRs (Fig. 2). It should be noted that the positively charged sequence of N-terminus of the NAC-β subunit from C. *elegans* was shown recently not only to be responsible for ribosome binding but also, being unstructured, has the ribosome independent chaperone activity[24].

Phosphorylation is regarded as one of the most common types of PTM in a long (> 100 aa) IDRs [25]. We used ELM (eukaryotic linear motif resource for functional sites in proteins, http://elm.eu.org) to predict phosphosites and docking motifs for protein kinases along the gNAC-β and gNAC-α sequences in comparison with the ubiquitous paralogs (Fig. 2), as well as for several distinct gNACβ paralogs (Fig. 2 and Fig. 3). This analysis show that IDRs in checked proteins are predicted to have numerous putative phosphosites for *Drosophila* protein kinases (Fig. 2). We also traced the diversity of the predicted phosphosites (Fig. 3) by comparing four highly homologous copies of gNAC-β gene [9] (Fig. 3). The bNACtes4 demonstrates the emergence of phosphosite within the newly acquired amino acid stretch and acquisition of the adjacent phosphosite. At the same time, two phosphosites were lost from the very

bNACtes4 C-terminus, comparative to the other three copies. Prior to directly demonstrate paralog phosphorylation, we performed a rough evaluation of the abundances of their transcripts using testis polyA mRNA NGS sequencing. We estimated the relative abundances of paralogous gNAC-β mRNAs, which turned out to be comparable, showing slightly higher abundances for the bNACtes3,4 and 6 (the abundances of corresponding mRNAs in TPM looks as tes4 (19.8), tes3 and tes6 (15.9), tes1 and 2 (equal, 7.5), tes 5, pseudogene, (1.0)). We've checked whether gNAC proteins are phosphorylated *in vivo*. We performed 2D electrophoresis, using isoelectrofocusing in the first direction and revealed, by immunodetection, the extremely heterogeneous profile of the gNACβ proteins in the extracts of testis ribosomes. The observed pI range of the major spots of gNAC-β proteins is 6.5-8, which is significantly lower than the theoretically predicted 9.15-10 (from Polypeptide Report of the Flybase) for the distinct NAC-β germinal paralogs. Correspondingly, the phosphatase treatment of the ribosomal extract resulted in the vanishing of spots from the more acidic region and drastic shifts of the gNAC-β spots pattern toward alkaline pI values (Fig. 4a, b). This phosphatase-dependent diminishing of the spots corresponds to a more acidic pI region demonstrating gNAC-β subunits phosphorylation. The number of the detected spots (at least nine) is higher than the number of expressed paralogs (five), indicating the existence of dynamic alternatively phosphorylated states of germinal paralogs.

Functional crosstalk between the ubiquitous and germinal subunits of NAC

The question arises about the possible functional interchangeability of the ubiquitous and germinal NAC subunits functions, in particular, the ability of the NAC-α/gNAC-β chimeric heterodimer to provide at least some of the diverse functions of ubiquitous NAC. To test this, we evaluated the ability of the ectopic expression of gNAC-β subunit to rescue the lethal mutation of the *bic* [17], which encodes the ubiquitously expressed NAC-β subunit. For this, we generated fly strains with genomic insertions of transgene encoding gNAC-β driven by the actin5C promoter and checked whether these transgenes are able to suppress the lethal effect of the null *bic*^{1} gene mutation [17] (Fig. 5). Transgene insertions into chromosomes 2 (T2) and 3 (T3) were shown to provide high and medium levels of gNAC-β expression, respectively, as assessed by WB analysis (Fig. 5a). T3 showed no visible suppressive effect (Fig. 5b), while T2 ensured the survival of up to 30% of fertile individuals. We hypothesize that gNAC-β protein, which carries the additionally acquired C-end IDR sequence, is able of performing some functions of the ubiquitous NAC-β subunit in chimeric NAC-α gNAC-β heterodimer. On the other hand, we identified an indication of the role of the ubiquitous NAC-α subunit in determination of gonad development and maintaining of fertility. The separate germinal RNAi KD of ubiquitous *NAC-α* or germinal *NAC-α* exert no visual phenotypes while their simultaneous combination led to the strong disturbance of gonad development and infertility (Fig. 6, c and d, see legend) without affecting fly viability.

The germinal and ubiquitous NAC paralogs in the genomes of related species

The evolutionary origins of paralogous ubiquitous and germinal pairs of NAC proteins attract an interest not only due to IDRs acquirement by germinal paralogs but also in connection of our observation of specific «functional crosstalk's» between the germinal and ubiquitous paralogs being a topic of discussions concerning evolution of paralogs, especially those capable to form heterodimers [26]. We constructed the phylogenetic tree of 69 *Drosophilidae* species whose genomic assemblies were downloaded from the NCBI. The assemblies were subjected to BUSCO analysis [27] to identify universal single copy orthologs followed by their multiple alignments and the construction of the phylogenetic tree of *Drosophila* species. The generated phylogenetic tree is in good agreement with others previously reported (Fig. 7) (e.g. «*Drosophila* 25 Species Phylogeny» 2017 Dataset posted on 28.09.2017). We found that the genomes of all mentioned species from the *Sophophora* subgenus, diverged from a common ancestor ~ 27 Mya, encode both ubiquitously and germinal-expressed NAC-α as well as ubiquitous NAC-β genes, while the amplified *gNAC-β* genes are found in the *melanogaster* group genomes, but not in *obscura* group. We also identified the *gNAC-β-like* genes carrying extended IDRs in the genomes of earlier branched-off species, *D. willistoni* and *D. busckii*. These IDRs presented by comparable lengths to those in D. *melanogaster* are characterized by much more orthologous divergencies than the NAC domain sequences (Fig.S1). Interestingly, despite a high level of the orthologous polymorphism, the distribution of S/T locations in the region of predicted phosphosites was shown to be positionally conserved comparing IDR orthologous sequences from *D. willistoni* and *D. melanogaster*. The comparison of corresponding sequences encompassing ~ 50 amino acid stretches (Fig.S1) reveals conservative locations of six S/T positions marked by a red line with crosses (Fig.S1) intermingled with the rest of multiple amino acid substitutions. The detection of conservative positions of putative functional phosphosites in orthologous IDR sequences is in accord with the notion that IDRs are conserved across orthologs in the vast majority of cases [28] as well as the recent report of conservative RNA binding domains positions in the orthologous pairs of IDRs, including the *Drosophila* and human pairs [29]. In the orthologous pair of IDR sequences of earlier branchedoff species, *D. willistoni* and D. *busckii*, albeit a shift of serine enriched cluster along amino acid sequence, we also identified three conservative serine positions (Fig.S1, red circles).

The numbers of ubiquitous NAC-α and NAC-β copies are shown to be correlated with each other in most species belonging to the *montium* subgroup of the *melanogaster* group (Fig. 7). This observation is consistent with the earlier report on the production of equimolecular α- and β-subunits in yeast cells [30]. It should be noted that the correspondence between gene numbers of the germinal α- and β-subunits is lost in several species from the *melanogaster* group, which are characterized by the amplification of the gNAC-β genes (Fig. 7).

The phylogenetic analysis of NAC homologs revealed that besides gNAC-β and ubiquitously NAC-β there is a third large family of NAC-β proteins (Fig.S2), named here as uncNAC-β (*unc*haracterized, *CG11835* Flybase.org). Almost all species, except *D. punjabiensis* (Fig. 7), contain a single copy of *uncNAC-β* (*melanogaster* gene structure is presented in Fig. 2) encoding the NAC domain followed by about 800 amino acid residues of an extremely extended IDR. Here the orthologous IDRs comparison reveals the clusters of conservative proline dependent protein kinase phosphosites that are concentrated at the C-

ends of uncNAC-β proteins (Fig.S2). Although the putative partners of uncNAC-β remain to be elucidated, we may suggest its heterodimerization with NAC-α subunits is capable to transfer some functionally important properties to newly formed heterodimers.

The cross-species alignment (Fig. S3, Data Set 1) shows that the ubiquitous NAC-α domains are very conserved, while the gNAC-α domains are diverged slightly faster (the average amino acid identity per column for multiple alignments of NAC domains is 80% and 75.6% for the ubiquitous and gNAC-α, respectively). The same feature is even more noticeable for the orthologous pairs of the NAC-β ubiquitous and germinal counterparts (the average identity per column in the multiple alignments of NAC domains is 69.4% and 38.8% for ubiquitous and germline NAC-β domains, respectively). These values for the multiple alignments of the overall IDR sequences for gNAC-β is 8%, while the distinct regions within IDR reach the average identity of 50% indicating significant conservation. Of note, some species subgroups from *Sophophora* subgenus have several highly similar paralogs of the αNAC and/or βNAC subfamilies.

Discussion

Earlier, we have described the five copies of testes-expressed highly homologous genes encoding β-subunits of ribosome associated NAC in the *D. melanogaster* genome [9,10,15]. These genes are localized in the distinct 12E region in the X-chromosome and designates in Flybase data as *betaNACtes1*, and two adjacent pairs of genes, *betaNACtes* 2,6 and *betaNACtes* 3,4 [10]. As far as we know, we found for the first time [10] the presence of tissue-specific subunit of NAC in multicellular eukaryotes that is thought to be involved in protein homeostasis [2,3]. Here, we discovered the germinal NAC-αβ paralog, whose α-subunit is expressed exclusively in the germline during early embryonic development. In this paper, we also characterized the expression of germinal-specific gNAC-α and gNAC-β-subunits during early embryonic development of *D. melanogaster*, this allows us to use the designation “gNAC” for germinal specific heterodimeric gNACs. Earlier, we failed to observe the negative effect of siRNA *βNACtes* KD on fertility in testes, possibly due to incomplete depletion of mRNAs of these amplified genes [9]. The identification of a unique gene for the gNAC-α subunit, presented in this paper, opens the way for the elimination of gNAC protein activity using CRISPR/Cas9 gene editing to trace the putative negative fertile effect.

Comparison of the amino acid sequence patterns of the ubiquitous and germinal NAC subunits revealed significantly extended IDRs at the C- and N-ends of the β- and α- subunits of gNAC, respectively. The burst of the interest to IDRs is explained by a large amount of recently accumulated data demonstrating the functional role of IDRs, their role in protein-protein interactions and the formation of biocondensates [31,32]. It is known that IDRs are protein unfolded parts that provide protein-protein interactions [33] that are considered to be necessary to perform ubiquitous NAC function and its chaperone activity in *C. elegans* [24], and we suggest that germinal-specific evolutionary acquired IDR sequences participate in the sophisticated germline protein-specific interactions. Here we detected the presence of phosphorylated isoforms of germinal NAC-β subunits. We also predicted the excess of phosphorylation sites (phosphosites) at the extended IDRs of gNAC subunits compared to the ubiquitous paralogs. Taking into

account the important role of NAC with its flexible adaptor sites ensuring interactions between the nascent polypeptide and components of the protein sorting machinery [1,2] and functional conformational mobility of phosphorylated IDRs [34,35], the in-depth experimental studies of NAC phosphorylation will be necessary to discern the peculiarities of their functions in somatic and germinal cells. However, it remains a challenge to associate these IDR regions with specific biological and biochemical functions based on their amino acid sequences and putative PTM sites [36].

The detection of specific NAC in the germline is of particular interest, considering some peculiarities of protein synthesis regulation in the germline development, associated with proliferation and differentiation programs [37]. We suggest that the germinal NAC subunits, carrying the extended flexible and easily accessible for PTM amino acid sequences can be used in the germline proteostasis regulation. The recent *in vitro* study of human βNAC function using reticulocyte rabbit ribosomes has revealed a novel NAC function as a component of the ternary complex «NAC-ribosome nascent chain complex-SRP with SR-receptor» located at the ribosomal exit site [3,38]. The authors found ubiquitous NAC to perform selective biasing the flexible conformational landscape of multicomponent SRP for association with its receptor during the cotranslational targeting the N-terminal signal carrying nascent polypeptide to ER. Thus, a more active and broader role of ubiquitous NAC in protein synthesis as an allosteric regulator of SRP [24] emphasize the assumption that specific interactions involving IDRs of both gNAC subunits can be functional in the germline.

Here we found that the lethal effect of the lack of ubiquitous NAC-β subunit is rescued by the ectopically expressed paralog carrying IDRs. This observation does not mean a possibility of a replacing the ubiquitous heterodimer with a germinal paralog, since the effectiveness of the chimeric gNACβ-NAC-α heterodimer in the implementation of protein homeostasis has not been evaluated. The observed suppression indicates only a certain level of functional flexibility of the heterodimer subunits. Nevertheless, here we found the presence of functional crosstalk's between the ubiquitous and germinal paralogs of both α and β subunits of NAC. This type of crosstalk is known to be accompanied by a well-known asymmetric evolution (subfunctionalization) of paralogs [39] without a violating of a possibility of their interchangeability. We suppose these functional crosstalk's may be beneficial to maintain reproduction system based on germinal cell proteome robustness. This type of paralogous interactions was shown to be especially related to the cases of paralogs capable to form heterodimers [40] that is occurred for the subunits of NAC paralogs.

The switch-like decisions during germ cell development are proposed to be closely related to the formation of large protein complexes, including large granules, also known as membraneless organelles (for review [41,42]). In this regard, new ideas about the cotranslational assembly of multisubunit protein complexes with the participation of a chaperone, based on rigorous experiments, are of particular interest [2,43–45]. The authors propose that the translations of subunit complexes are spatially confined. These ideas are discussed in the terms of compartmentalized translation principles with regulatory implications in development [46,47]. It would be attractive to extend such concepts to the description of the complex

processes of granule formation in the germ plasm compartment of a mature oocyte in which, according on our preliminary experiments, gNAC participates. However, for now, the identification of gNAC only opens the door to the first experimental approaches to explore its functions.

Methods

Fly stocks and crosses

Batumi line laboratory stock was used in biochemical experiments and immunostaining. To generate recombinant chromosome 2 carrying the *bic* [1] lethal allele and FLAG.gNACβ transgene, the *y*[1]*w*; Eney-whited700- pAc5.1.FLAG.gNAC*-β.*RetMI07200/ CyRoi* females were crossed to *bic*[1]*L*[2]*/CyRoi* males and the F1 *Eney-whited700- pAc5.1.FLAG.* g*NAC*-β.*RetMI07200/ bic*[1]*L*[2] females were crossed to *yw*[67c23], +/+ males. Male progeny of this cross with recombinant chromosome (marked *whited700* and *L*[2]) *Eney-whited700- pAc5.1.FLAG.gNAC*-β.*RetMI07200 bic*[1]*L*[2]/+ were collected and individually crossed to *yw*[67c23], +/ *CyRoi* females. Males *Eney-whited700- pAc5.1.FLAG.gNAC*-β.*RetMI07200 bic*[1]*L*[2]*/CyRoi* were crossed to *bic*[1]*L*[2]*/CyRoi* females and the viable *Eney-whited700- pAc5.1.FLAG.gNAC*-β.*RetMI07200 bic*[1]*L*[2]*/ bic*[1]*L*[2] individuals (lacking *CyRoi* and carrying the *whited700* and *L* markers) were traced/selected to evaluate the suppression effect of the *bic*[1] lethality.

Germinal knockdowns

nos-Gal4 > UAS-gNACα-RNAi and *nos-Gal4 > UAS-ubNACα-RNAi* (VDRC) were performed separately or simultaneously using *nos-Gal4 > UAS-gNACα-ubNACα-RNAi.* The driver line was obtained from Bloomington Stock #25751, *P{UAS-Dcr-2,D}1,w*[1118]; *P{GAL4-nos,NGT}40*. RNAi lines include stocks from VDRC: # 102621 (gNACα (*CG4415*)), and # 36017 (ubiquitous NACα (*CG8759*)).

Constructs of plasmids

RT-PCR products of gNAC-β and gNAC-α ORFs were inserted into pAc5.1. FLAG or pAc5.1.HA carrying plasmids. Oligos for plasmid insertions:

pAc5.1.FLAG.gNAC-β (CG18313)

Xho1- 5'tataCTCGAGACAATGGATTTCAACAAGCGACAG

Apa1- 5' tataGGGCCCCTAATCTTCGTCCTCGGAGACCT ;

pAc5.1.HA.gNAC-α (CG4415):

Kpn1-5'tataGGTACCTTCCTCAAGATGGGTAAGAAGCAGA

Xho1- 5' tataCTCGAGGTTGTCGTTCTTCAGCAGCGC

Generation of transgenic lines expressing FLAG.gNACβ protein under pAc5.1 promoter

Transgenic strains carrying construct *attBs-Eney-whited700- pAc5.1.FLAG.gNAC-β-attBsrev-pSK = aeca* were generated by *phiC31*-mediated site-specific integration at the MiMIC site [48–50] in the *Ret* gene of chromosome 2 (Bloomington #43099, *y1w*; MiRetMI07200/SM6a*) and at the site (Bloomington #24862, *yM{RFP[3xP3.PB] GFP[E.3xP3] = vas-int.Dm}ZH-2A w[*]; PBac{y[+]-attP-9A}VK00005*) of chromosome 3. The *vas-dPhiC31* strain bearing the *phiC31* gene under the control of the *vasa* gene promoter on the X chromosome was used as an integrase source [49]. The germ-line transformation of the embryos was performed according to standard protocol [51] with the approximately 40% efficiency of integration.

Generation of antibodies against germinal NACβ subunit

Here we generated rabbit anti His-tagged germinal NAC-β subunit antibodies using antigen sample as earlier described [10]. Antibodies were purified by antigen affinity chromatography using Thermo Scientific AminoLink Plus Coupling Resin according to the manufacturer's protocol (Thermo Fisher Scientific). The generated antiserum was shown to recognize exclusively the germ cells in testes and early embryos and was used in Western-blot analysis (dilution 1:1000).

Cell culture transfection, immunoprecipitation, and western-blot analysis

Transient transfections of S2 cells were performed with the help of FuGENE® HD Transfection Reagent (Promega# E2311) according to the manufacturer's instructions. 3–4 days after transfection cells were harvested and subjected to immunostaining. For immunoprecipitation, anti-HA Magnetic Beads (#88836 Thermo Scientific) or anti-FLAG M2 Magnetic Beads (M8823 Sigma) were used. Protein samples (S2 cells or fly extracts) were applied to SDS-PAGE, transferred onto PVDF membrane according to standard protocols. The blots were analyzed using antibodies in a dilution 1:1000 against germinal NACβ, monoclonal mouse anti-FLAG M2 (Sigma F3165) and monoclonal mouse anti HA-Tag antibodies (mAB#2367 Cell Signalling Tech). Alkaline-phosphatase-conjugated anti-rabbit or anti-mouse antibodies (Sigma) were used as secondary reagent at a dilution of 1:20,000. Blots were developed using the Immun-Star AP detection system (Bio-Rad Laboratories) in accordance with the recommendations of the manufacturer, signal was detected using the BioRad Chemi Doc MP Imaging System.

Ribosome's isolation and 2D resolution of ribosomal proteins from testis

250 pairs of frozen testes were homogenized in a Dounce homogenizer in 1,5 ml of buffer containing 25mM Hepes [pH7.6], 100mM KCl, 5mM MgCl2, 1mM DTT, RNase inhibitor RiboLock (Thermo Scientific) at 40 units/ml, 0.015% digitonin, 1% NP-40, 0.5% sodium deoxycholate and 100 µg/ml cycloheximide. A protease inhibitor cocktail was used, as recommended by the company (Protease Inhibitor Cocktail Tablets, Roche). Cell fragments and mitochondria were removed by centrifugation at 12000g at 4^{o}C for

20 min as described earlier [9]. 1,5 ml post-mitochondrial extract was centrifugated for 1 hour at 35,000 RPM (100000g) in a rotor Himac P50A3-0529, ultracentrifuge CP100-NX, at 4^{o}C. 2D electrophoresis was performed at the «Human Proteome» Collective Use Center of the V.N. Orekhovich Federal State Budgetary Scientific Institution Research Institute of Biomedical Chemistry.

For first dimension, ribosome pellet or protein precipitate after dephosphorylation were suspended in 250 µl of buffer (7M urea, 2M thiourea, 4% [w/v] CHAPS, 1% [w/v] DTT, 2% immobilized pH gradient [IPG] buffer [pH 3–10], protease and phosphatase inhibitor cocktails [Roche Diagnostics, Mannheim, Germany]), then clarified for 10 min at 10000 g at 4°C. 120 µl of clarified protein solution mixed with 30 µl of rehydration buffer (7M urea, 2M thiourea, 2% CHAPS ,0.3% DTT, 0.5% IPG buffer [pH 3–11 NL], and 0.001% bromophenol blue) was used to prepare first-dimensional gel. 7-cm IPG gel strips (pH3-10) were rehydrated passively for 10 hour at 4°C. IEF was conducted at 20°C using Protean IEF Cell (“Bio-Rad”). Power supply was programmed in the gradient mode with voltages for four steps: first – 300V (00.30 min), second - gradient 1000V (00.30min), third – gradient 5000V (01.20min), fourth and hold – 5000V (00.25 min). Prior to the second dimension, the IPG gel strip was soaked for 10 min in equilibration solution 950 mM Tris-HCL [pH6.8], 6M urea, 2% SDS, 30% glycerol) containing 1% DTT. This process was followed by a 10-min incubation in the equilibration solution containing 5% iodacetamide. IPG gel strip was then placed on top of the second-dimensional stab gel and sealed using 1 ml of molten agarose with 0.5% TGS electrode buffer (24 mM Tris [pH8.3], 200 mM glycine, and 0,1% SDS). The second dimension SDS-PAGE was carried out using Hoefer miniVE vertical electrophoresis system [12% w/v gel concentration, 80 × 90 × 1 мм in size]. Precision Plus Protein Standards (BioRad) was used as a marker. Electrophoresis was performed at constant current (25 mA/gel) and 100 to 160 V for 1.5 h at room temperature. On completion of electrophoresis, the gel was rinsed in transfer buffer (48 mM Tris, 39 mM glycine, 0.037% SDS, and 20% methanol) and transferred to a PVDF membrane using a semidry transfer cell (Bio-Rad) following the manufacturer’s instructions.

Ribosome treatment by Calf Intestinal (CIP Sigma #4978) Alkaline Phosphatase

The treatment was performed according to following protocol: ribosomal pellet from 125 testes was suspended in 1xCIP buffer (0,1M NaCl, 0,05M Tris-HCl pH 7,9, 0,01M $MgCl_2$, 1 mM DTT) ,1 x Tm Complete protease inhibitor mix (Roche), 20 units CIP, and reaction mix was incubated 120 min at 37^{o}C. Dephosphorylation was completed by addition cold 10% trichloroacetic acid. Precipitate was washed twice by acetone before isoelectrofocusing.

Immunostaining

12–15-hour embryos were collected, dechorionated in bleach (2%) for 3 minutes and after thorough rinsing with water were devitellinized in a 1:1 heptane/methanol mixture (-20°C) in a 1.5 ml microtube by gently shaking. Devitellinized embryos sinking in the methanol phase, were then rinsed 3 times with cold methanol. Embryos can be stored at -20°C until immunostaining. For immunostaining, embryos were gradually rehydrated with methanol-PBT (PBS with 0,1% Tween20), washed 3 times with PBTX (PBT with

0,3%Triton X100) and permeabilized in PBTX with 0,3% sodium deoxycholate (Sigma) for one hour. Then embryos were washed three times in PBTX and blocked with PBTX containing 5% normal goat serum (NGS, Invitrogen) for 1 hour. Embryos then were incubated first in specific primary antibodies in PBTX containing 3% NGS overnight at + 4°C and after washing 4 times in PBTX at room temperature, incubated the next overnight at + 4°C with secondary antibodies labeled with Alexa in a dark chamber. Embryos were mounted in Invitrogen SlowFade Gold Antifade reagent. The following primary antibodies were used: rabbit polyclonal anti-gNACβ (1:500), rat anti-VASA (1:200) (DSGB: AB_760351). Secondary antibodies were anti-rabbit IgG Alexa Fluor 546; anti-rat IgG Alexa Fluor 488 (Invitrogen, Thermo Fisher Scientific). Confocal microscopy was done using Zeiss LSM 900.

Testes and ovaries of adult (1–2 day old) males and females were dissected in phosphate-buffered saline (PBS) at 4°C, washed with PBT, fixed in 3.7% formaldehyde in PBT for 30 min at room temperature and then were processed and immunostained like embryos.

Quantification of NACs mRNA abundances

The abundances of testis-specific NACs were calculated by Salmon Galaxy ver. 1.5.1 using R6.22 transcripts fasta file and default settings. The source datasets and sequencing conditions are available in NCBI GEO, accession GSE101060.

Phylogeny of 69 Drosophila species

To estimate the phylogeny of *Drosophila* species, the 192 RefSeq and GenBank genomic assemblies of 70 species were downloaded from the NCBI. Each assembly was subjected to BUSCO v.4.1.4 [27] analysis to identify the universal single-copy orthologs from OrthoDB (-l dipteria_odb10). The genomic assembly of *Musca domestica* (GCF_000371365.1_Musca_domestica-2.0.2) was also analyzed by BUSCO for further usage as the outgroup. 3,119 universal single-copy BUSCO orthologs that are present in at least 90% of 192 assemblies and 69 genomic assemblies (one assembly per species) having at least 90% of 3,119 single-copy orthologs were selected for the *Drosophilidae* phylogenetic analysis and the identification of NAC family proteins (Table S1). The concatenated multiple sequence alignments of the orthologous proteins (using MAFFT v7.471[52] followed by alignment trimming with trimAl v.1.4 [53] (-gt 0.5) resulted in 710,094 amino acid columns that were used to estimate the maximum likelihood species phylogeny using RAxML v.8.0 [54] with the PROTGAMMAJTT model, rooted with the *Musca domestica*. We then used r8s [55] to estimate branch lengths in terms of millions of years with four calibration points [56] 25–30 million of years (moy) for the common ancestor of *D. pseudoobscura* and *D. melanogaster*, 40 moy for the common ancestor of *D. virilis* and *D. melanogaster*, 6–15 moy for the common ancestor of *D. yakuba* and *D. melanogaster*, and 100 moy for the common ancestor of *D. melanogaster* and *Musca domestica*.

The identification of NAC family proteins

The initial identification of NAC genes in *Drosophilidae* genomic assemblies was performed with *tblastn* v. 2.6.0 [57] (-evalue 10E-5) using NAC proteins from *D. melanogaster* as the queries. The hit regions

extended with the additional 2000 bp on both sides were extracted from the genomes and were subjected to the determination of the open reading frames by AUGUSTUS v. 3.1.3 [58]. The identified open reading frames were confirmed as encoding NAC domains using InterProScan v.5.39 [59] (IPR016641 for αNAC and IPR039370 for βNAC). If the analyzed genome was already annotated by the NCBI (40 genomic assemblies), then the accession number of the proteins was determined by *blastp* against the corresponding proteoms retrieved from the NCBI Protein database; otherwise (29 assemblies) the NAC protein was marked as 'novel'. The multiple alignments of NAC proteins were carried out by the MAFFT v. 7.471[52]. The NAC domains of αNAC and βNAC were cut from the alignments and the positions including greater than > = 0.5 gaps were removed by trimAl, v.1.4 [53]. Phylogenetic analysis of NAC domains was performed using the FastTree program [60] with default parameters, with the WAG evolutionary model and the discrete gamma model with 20 rate categories. The tree structure was validated with bootstrap analysis (n = 100).

Declarations

Acknowledgments

We thank O. Maksimenko for her help and advice in generation of rabbit antibodies to the gNAC-β protein, E. Zorina for providing 2D electrophoresis and V. Velkov for his input in this manuscript. This work was supported by a research grant from the Russian Science Foundation (RSF) (grant number 19-74-20178).

Author contributions

G.K. conceived and performed most of the experiments; O.O. and Yu.A. generated the transgenic drosophila lines; T.L. carried out antibody generation and purification; E.M. conducted cell culture transfection and immunostaining; S.R. have performed the phylogenetic analysis; O.G. searched the IDR in the NAC proteins; N.A. performed Western-blot and IP analysis; S.L. performed RNAseq analysis, V.G. designed the project and wrote the manuscript.

Data availability statement

The alignments used for the phylogeny are presented in Supplementary materials. NGS datasets are deposited to NCBI GEO, accession GSE101060. Materials (fly lines, etc.) from the paper are available upon request.

Competing Interests Statement

The authors have no competing interests or other interests that might be perceived to influence the results and/or discussion reported in this paper. All authors gave final approval for publication and agree to be held accountable for the work performed therein.

References

1. Deuerling, E., Gamerdinger, M. & Kreft, S. G. Chaperone Interactions at the Ribosome. Cold Spring Harb Perspect Biol **11**, doi:10.1101/cshperspect.a033977 (2019).
2. Kramer, G., Shiber, A. & Bukau, B. Mechanisms of Cotranslational Maturation of Newly Synthesized Proteins. Annu Rev Biochem **88**, 337–364, doi:10.1146/annurev-biochem-013118-111717 (2019).
3. Hsieh, H. H. & Shan, S. O. Fidelity of Cotranslational Protein Targeting to the Endoplasmic Reticulum. Int J Mol Sci **23**, doi:10.3390/ijms23010281 (2021).
4. del Alamo, M. *et al.* Defining the specificity of cotranslationally acting chaperones by systematic analysis of mRNAs associated with ribosome-nascent chain complexes. PLoS Biol **9**, e1001100, doi:10.1371/journal.pbio.1001100 (2011).
5. Wegrzyn, R. D. & Deuerling, E. Molecular guardians for newborn proteins: ribosome-associated chaperones and their role in protein folding. Cell Mol Life Sci **62**, 2727–2738, doi:10.1007/s00018-005-5292-z (2005).
6. Yogev, O., Karniely, S. & Pines, O. Translation-coupled translocation of yeast fumarase into mitochondria in vivo. J Biol Chem **282**, 29222–29229, doi:10.1074/jbc.M704201200 (2007).
7. Gamerdinger, M. *et al.* Early Scanning of Nascent Polypeptides inside the Ribosomal Tunnel by NAC. *Mol Cell* **75**, 996–1006 e1008, doi:10.1016/j.molcel.2019.06.030 (2019).
8. Jomaa, A. *et al.* Mechanism of signal sequence handover from NAC to SRP on ribosomes during ER-protein targeting. Science **375**, 839–844, doi:10.1126/science.abl6459 (2022).
9. Kogan, G. L., Usakin, L. A., Ryazansky, S. S. & Gvozdev, V. A. Expansion and evolution of the X-linked testis specific multigene families in the melanogaster species subgroup. PLoS One **7**, e37738, doi:10.1371/journal.pone.0037738 (2012).
10. Kogan, G. L. *et al.* [Nascent Polypeptide-Associated Complex as Tissue-Specific Cofactor during Germinal Cell Differentiation in Drosophila Testes]. Mol Biol (Mosk) **51**, 677–682, doi:10.7868/S0026898417040115 (2017).
11. Bardwell, J. C. & Jakob, U. Conditional disorder in chaperone action. Trends Biochem Sci **37**, 517–525, doi:10.1016/j.tibs.2012.08.006 (2012).
12. Tompa, P. & Kovacs, D. Intrinsically disordered chaperones in plants and animals. Biochem Cell Biol **88**, 167–174, doi:10.1139/o09-163 (2010).
13. Bah, A. *et al.* Folding of an intrinsically disordered protein by phosphorylation as a regulatory switch. Nature **519**, 106–109, doi:10.1038/nature13999 (2015).
14. Borgia, A. *et al.* Extreme disorder in an ultrahigh-affinity protein complex. Nature **555**, 61–66, doi:10.1038/nature25762 (2018).
15. Usakin, L. A., Kogan, G. L., Kalmykova, A. I. & Gvozdev, V. A. An alien promoter capture as a primary step of the evolution of testes-expressed repeats in the Drosophila melanogaster genome. Mol Biol Evol **22**, 1555–1560, doi:10.1093/molbev/msi147 (2005).
16. Larkin, A. *et al.* FlyBase: updates to the Drosophila melanogaster knowledge base. Nucleic Acids Res **49**, D899-D907, doi:10.1093/nar/gkaa1026 (2021).

17. Markesich, D. C., Gajewski, K. M., Nazimiec, M. E. & Beckingham, K. bicaudal encodes the Drosophila beta NAC homolog, a component of the ribosomal translational machinery*. Development **127**, 559–572 (2000).
18. Szklarczyk, D. *et al.* The STRING database in 2017: quality-controlled protein-protein association networks, made broadly accessible. Nucleic Acids Res **45**, D362-D368, doi:10.1093/nar/gkw937 (2017).
19. Lehmann, R. & Nusslein-Volhard, C. Abdominal segmentation, pole cell formation, and embryonic polarity require the localized activity of oskar, a maternal gene in Drosophila. Cell **47**, 141–152, doi:10.1016/0092-8674(86)90375-2 (1986).
20. Ephrussi, A. & Lehmann, R. Induction of germ cell formation by oskar. Nature **358**, 387–392, doi:10.1038/358387a0 (1992).
21. Martin, E. M. *et al.* Conformational flexibility within the nascent polypeptide-associated complex enables its interactions with structurally diverse client proteins. J Biol Chem **293**, 8554–8568, doi:10.1074/jbc.RA117.001568 (2018).
22. Lobanov, M. Y. & Galzitskaya, O. V. The Ising model for prediction of disordered residues from protein sequence alone. Phys Biol **8**, 035004, doi:10.1088/1478-3975/8/3/035004 (2011).
23. Lobanov, M. Y., Sokolovskiy, I. V. & Galzitskaya, O. V. IsUnstruct: prediction of the residue status to be ordered or disordered in the protein chain by a method based on the Ising model. J Biomol Struct Dyn **31**, 1034–1043, doi:10.1080/07391102.2012.718529 (2013).
24. Shen, K. *et al.* Dual Role of Ribosome-Binding Domain of NAC as a Potent Suppressor of Protein Aggregation and Aging-Related Proteinopathies. *Mol Cell* **74**, 729–741 e727, doi:10.1016/j.molcel.2019.03.012 (2019).
25. Koike, R. & Ota, M. All Atom Motion Tree detects side chain-related motions and their coupling with domain motion in proteins. Biophys Physicobiol **16**, 280–286, doi:10.2142/biophysico.16.0_280 (2019).
26. McClune, C. J. & Laub, M. T. Constraints on the expansion of paralogous protein families. Curr Biol **30**, R460-R464, doi:10.1016/j.cub.2020.02.075 (2020).
27. Seppey, M., Manni, M. & Zdobnov, E. M. BUSCO: Assessing Genome Assembly and Annotation Completeness. *Methods Mol Biol* 1962, 227–245, doi:10.1007/978-1-4939-9173-0_14 (2019).
28. Bellay, J. *et al.* Bringing order to protein disorder through comparative genomics and genetic interactions. Genome Biol **12**, R14, doi:10.1186/gb-2011-12-2-r14 (2011).
29. Panhale, A. *et al.* CAPRI enables comparison of evolutionarily conserved RNA interacting regions. Nat Commun **10**, 2682, doi:10.1038/s41467-019-10585-3 (2019).
30. Raue, U., Oellerer, S. & Rospert, S. Association of protein biogenesis factors at the yeast ribosomal tunnel exit is affected by the translational status and nascent polypeptide sequence. J Biol Chem **282**, 7809–7816, doi:10.1074/jbc.M611436200 (2007).
31. Chen, X. & Mayr, C. A working model for condensate RNA-binding proteins as matchmakers for protein complex assembly. RNA **28**, 76–87, doi:10.1261/rna.078995.121 (2022).

32. Wheeler, R. J. & Hyman, A. A. Controlling compartmentalization by non-membrane-bound organelles. Philos Trans R Soc Lond B Biol Sci **373**, doi:10.1098/rstb.2017.0193 (2018).
33. Borcherds, W., Bremer, A., Borgia, M. B. & Mittag, T. How do intrinsically disordered protein regions encode a driving force for liquid-liquid phase separation? Curr Opin Struct Biol **67**, 41–50, doi:10.1016/j.sbi.2020.09.004 (2021).
34. Tsang, B. *et al.* Phosphoregulated FMRP phase separation models activity-dependent translation through bidirectional control of mRNA granule formation. Proc Natl Acad Sci U S A **116**, 4218–4227, doi:10.1073/pnas.1814385116 (2019).
35. Bah, A. & Forman-Kay, J. D. Modulation of Intrinsically Disordered Protein Function by Post-translational Modifications. J Biol Chem **291**, 6696–6705, doi:10.1074/jbc.R115.695056 (2016).
36. Zarin, T. *et al.* Proteome-wide signatures of function in highly diverged intrinsically disordered regions. Elife **8**, doi:10.7554/eLife.46883 (2019).
37. Sanchez, C. G. *et al.* Regulation of Ribosome Biogenesis and Protein Synthesis Controls Germline Stem Cell Differentiation. Cell Stem Cell **18**, 276–290, doi:10.1016/j.stem.2015.11.004 (2016).
38. Hsieh, H. H., Lee, J. H., Chandrasekar, S. & Shan, S. O. A ribosome-associated chaperone enables substrate triage in a cotranslational protein targeting complex. Nat Commun **11**, 5840, doi:10.1038/s41467-020-19548-5 (2020).
39. Pich, I. R. O. & Kondrashov, F. A. Long-term asymmetrical acceleration of protein evolution after gene duplication. Genome Biol Evol **6**, 1949–1955, doi:10.1093/gbe/evu159 (2014).
40. Dandage, R. & Landry, C. R. Paralog dependency indirectly affects the robustness of human cells. Mol Syst Biol **15**, e8871, doi:10.15252/msb.20198871 (2019).
41. Dodson, A. E. & Kennedy, S. Phase Separation in Germ Cells and Development. Dev Cell **55**, 4–17, doi:10.1016/j.devcel.2020.09.004 (2020).
42. Lehmann, R. Germ Plasm Biogenesis–An Oskar-Centric Perspective. Curr Top Dev Biol **116**, 679–707, doi:10.1016/bs.ctdb.2015.11.024 (2016).
43. Rosenzweig, R., Nillegoda, N. B., Mayer, M. P. & Bukau, B. The Hsp70 chaperone network. Nat Rev Mol Cell Biol **20**, 665–680, doi:10.1038/s41580-019-0133-3 (2019).
44. Shiber, A. *et al.* Cotranslational assembly of protein complexes in eukaryotes revealed by ribosome profiling. Nature **561**, 268–272, doi:10.1038/s41586-018-0462-y (2018).
45. Chouaib, R. *et al.* A Dual Protein-mRNA Localization Screen Reveals Compartmentalized Translation and Widespread Co-translational RNA Targeting. *Dev Cell* **54**, 773–791 e775, doi:10.1016/j.devcel.2020.07.010 (2020).
46. Chin, A. & Lecuyer, E. Translating Messages in Different Neighborhoods. Dev Cell **54**, 691–693, doi:10.1016/j.devcel.2020.09.006 (2020).
47. Collart, M. A. & Weiss, B. Ribosome pausing, a dangerous necessity for co-translational events. Nucleic Acids Res **48**, 1043–1055, doi:10.1093/nar/gkz763 (2020).

48. Groth, A. C., Fish, M., Nusse, R. & Calos, M. P. Construction of transgenic Drosophila by using the site-specific integrase from phage phiC31. Genetics **166**, 1775–1782, doi:10.1534/genetics.166.4.1775 (2004).
49. Bischof, J., Maeda, R. K., Hediger, M., Karch, F. & Basler, K. An optimized transgenesis system for Drosophila using germ-line-specific phiC31 integrases. Proc Natl Acad Sci U S A **104**, 3312–3317, doi:10.1073/pnas.0611511104 (2007).
50. Venken, K. J. *et al.* MiMIC: a highly versatile transposon insertion resource for engineering Drosophila melanogaster genes. Nat Methods **8**, 737–743, doi:10.1038/nmeth.1662 (2011).
51. Rubin, G. M. & Spradling, A. C. Genetic transformation of Drosophila with transposable element vectors. Science **218**, 348–353, doi:10.1126/science.6289436 (1982).
52. Katoh, K. & Standley, D. M. MAFFT multiple sequence alignment software version 7: improvements in performance and usability. Mol Biol Evol **30**, 772–780, doi:10.1093/molbev/mst010 (2013).
53. Capella-Gutierrez, S., Silla-Martinez, J. M. & Gabaldon, T. trimAl: a tool for automated alignment trimming in large-scale phylogenetic analyses. Bioinformatics **25**, 1972–1973, doi:10.1093/bioinformatics/btp348 (2009).
54. Stamatakis, A. RAxML version 8: a tool for phylogenetic analysis and post-analysis of large phylogenies. Bioinformatics **30**, 1312–1313, doi:10.1093/bioinformatics/btu033 (2014).
55. Sanderson, M. J. r8s: inferring absolute rates of molecular evolution and divergence times in the absence of a molecular clock. Bioinformatics **19**, 301–302, doi:10.1093/bioinformatics/19.2.301 (2003).
56. Piccin, A. *et al.* The clock gene period of the housefly, Musca domestica, rescues behavioral rhythmicity in Drosophila melanogaster. Evidence for intermolecular coevolution? *Genetics* **154**, 747–758, doi:10.1093/genetics/154.2.747 (2000).
57. Altschul, S. F. *et al.* Gapped BLAST and PSI-BLAST: a new generation of protein database search programs. Nucleic Acids Res **25**, 3389–3402, doi:10.1093/nar/25.17.3389 (1997).
58. Keller, O., Kollmar, M., Stanke, M. & Waack, S. A novel hybrid gene prediction method employing protein multiple sequence alignments. Bioinformatics **27**, 757–763, doi:10.1093/bioinformatics/btr010 (2011).
59. Jones, P. *et al.* InterProScan 5: genome-scale protein function classification. Bioinformatics **30**, 1236–1240, doi:10.1093/bioinformatics/btu031 (2014).
60. Price, M. N., Dehal, P. S. & Arkin, A. P. FastTree 2–approximately maximum-likelihood trees for large alignments. PLoS One **5**, e9490, doi:10.1371/journal.pone.0009490 (2010).
61. Hu, Y. *et al.* iProteinDB: An Integrative Database of Drosophila Post-translational Modifications. G3 (Bethesda) **9**, 1–11, doi:10.1534/g3.118.200637 (2019).

Figures

Figure 1

Detection of gNAC-α/gNAC-β heterodimer in S2 cells and gNAC-β in embryo. a, Transfection of S2 cells for the expression of pAc5.1 gNAC-αHA and pAc5.1 FLAGgNAC-β plasmids encoding corresponding NAC subunits. b, Generation and detection of gNAC after Western-blot analysis of heterodimers immunoprecipitated by abFLAG and abHA and detected using same abs. c, FISH-hybridization to detect *CG4415* and *CG32601* genes expression of 14th stage embryos (from BDGP *in situ* homepage, https://insitu.fruitfly.org). d, gNACβ immunostaining of primordial gonads; e-g, migrating primordial gonadal cells, VASA (germ cell marker) and gNACβ colocalization. h, oocytes, late stages of oogenesis, gNAC-β accumulations at the posterior poles of oocytes (arrow). i, strong staining of testis spermatocyte, gNAC unstain somatic accessory gland (DAPI stained, arrow) and testis tip (arrowhead).

Figure 2

Schematic representation of NAC containing polypeptides with the plot providing the distribution of disorder propensity. The ELM predicted phosphosites are marked by red circle lollipops, sites predicted by ELM and confirmed using iProtein DB [61] are marked by filled red circles.

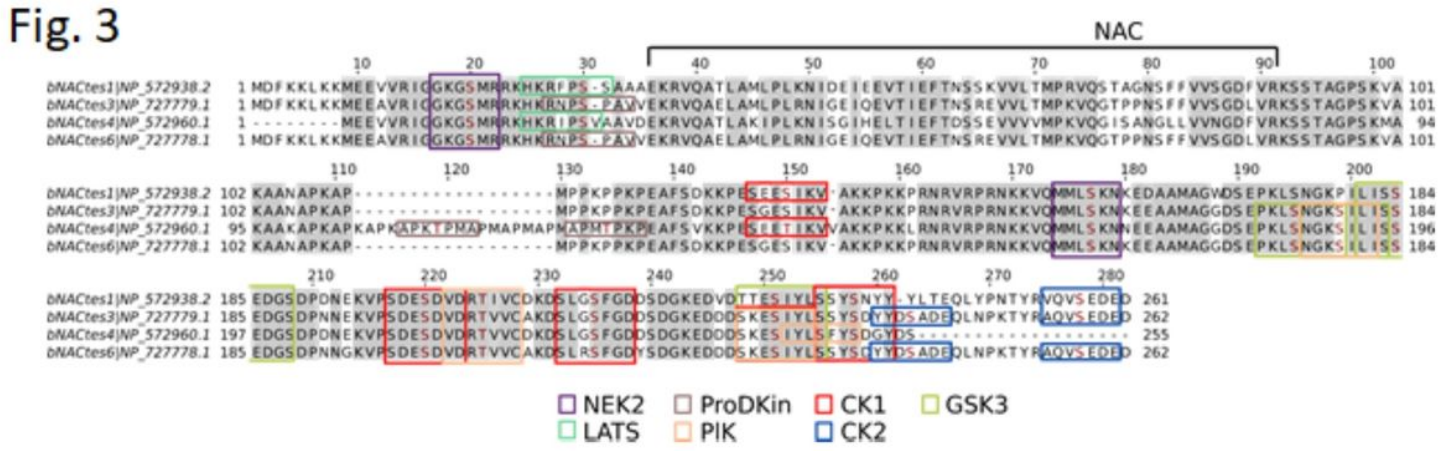

Figure 3

Predicted phosphosites in IDRs of the gNACβ subunits. Docking site for various Ser-Thr protein kinases (CK1, CK2, NEK2, LATS, ProDKin, PIK and GSK3-Ser) are indicated; X-linked paralogs of *D. melanogaster* (Flybase.org, ELM Database).

Figure 4

gNAC-β isoform spots from testis ribosomes before (a) and after alkaline phosphatase treatment (b), showing spots vanishing or shifting to a region with a higher pI.

Fig. 5

a

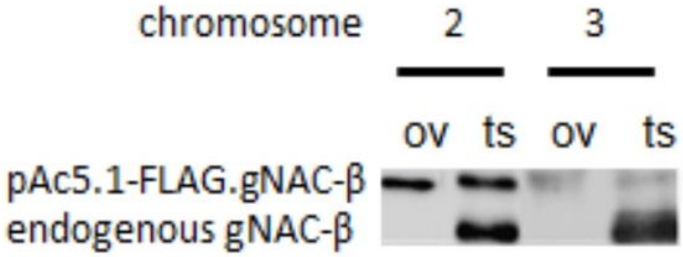

b

Genotype	viability
bic^{1}L^{2}/CyRoi	100%
bic^{1}L^{2}/bic^{1}L^{2}	<0,02%
bic^{1}L^{2}/CyRoi;P{pAc5.1.FLAG.gNAC-β}/TM3	100% T3
bic^{1}L^{2}/bic^{1}L^{2}; P{pAc5.1.FLAG.gNAC-β}/+	<0,2% T3
P{pAct5.1FLAG.gNAC-β}bic^{1}L^{2}/bic^{1}L^{2}	25-30% T2

Figure 5

The lethal phenotype of the *bic1* mutation caused by the loss of the ubiquitously expressed NAC-β is rescued by ectopic gNAC-β expression. a, Western blot analysis of FLAGgNAC-β transgenes (T2 and T3) expression inserted to chromosome 2 or 3, respectively. b, relative viability of the genotypes demonstrating transgene T2-induced suppression effect.

Figure 6

Germinal-specific siRNAi simultaneous knockdowns of both germinal and ubiquitous NACα disrupt the development of testis and oogenesis leading to complete infertility. DNA is stained with DAPI (blue), gNACβ (red), VASA (green). a, normal ovaries, arrow indicates stage 9 of oogenesis maturation and VASA expression in the nurse cells and posterior oocyte pole. b, normal testis, gNACβ immunostaining of spermatocytes, unstaining of somatic accessory glands (arrow) and seminal vesicles. c,d, adult ovaries and testis, images of double germinal knockdowns of germinal *(gNACα*) and ubiquitous *(ubNACα) NACα* genes using *nos-Gal4>UAS-gNACα-ubNACα-RNAi.*c, image of double germline knockdowns in ovaries

showing DAPI stained somatic residues of elongated ovarioles lacking germinal cells. d, elimination of germinal cells and testes, arrow points to the accessory gland, arrowhead to testis somatic remnant.

Figure 7

Phylogenetic tree of the Drosophila genus. The lack on this tree of some species (*mayri, watanabei, leontia, asahinai, pectinifera, obscura,montana, malanica and grimshawi*) is rather the result of the unfinished assembly of corresponding genomes preventing detection the NAC domain sequences. The number of paralogs is shown within shapes.

Supplementary Files

This is a list of supplementary files associated with this preprint. Click to download.

- SupFigures.zip